Mechanics and Energy
Mecânica e Energia

Numerical and experimental evaluation of the thermally stratified atmospheric boundary layer in wind tunnels

http://dx.doi.org/10.1590/0370-44672019740099

Renan de Souza Teixeira[1,4]
https://orcid.org/0000-0003-1700-6874
Daniel José Nahid Mansur Chalhub[2,5]
https://orcid.org/0000-0003-1956-5987
Pollyana de L. Massari[3,6]
https://orcid.org/0000-0002-8255-3682

[1]Universidade Federal Rural do Rio de Janeiro - UFRRJ, Departamento de Matemática - DEMAT, Seropédica - Rio de Janeiro – Brasil.

[2]Universidade do Estado do Rio de Janeiro – UERJ, Departamento de Engenharia Mecânica, Rio de Janeiro - Rio de Janeiro – Brasil.

[3]Pontifícia Universidade Católica do Rio de Janeiro - PUC-Rio, Departamento de Engenharia Mecânica, Rio de Janeiro - Rio de Janeiro – Brasil.

E-mails: [4]rsteixeira@ufrrj.br, [5]daniel.chalhub@eng.uerj.br, [6]pollyana.massari@gmail.com

Abstract

The atmospheric boundary layer (ABL) flow occurs due to the interaction between the Earth's surface and atmosphere, and it usually happens under thermal stratification. Therefore, in order to emulate this phenomenon, atmospheric wind tunnels need appropriate devices, such as spires and cubical roughness elements, at the entrance of the wind tunnel to create atmospheric characteristics for the analysis. In the current study, numerical and experimental investigations of the thermally stratified boundary layer are performed. The experimental data are measured using Inmetro's atmospheric wind tunnel. Two different spires set configurations and inlet velocities are considered. Moreover, the compressible Navier-Stokes equations using the k-epsilon turbulence model are computed by OpenFOAM opensource software. The simulated results and measured data presented a good overall agreement and showed that the proposed configuration provides the desired thermal and dynamic boundary layer necessary for the study of ABL.

Keywords: atmospheric boundary layer, Reynolds-averaged Navier–Stokes, heat transfer, computational fluid dynamics.

1. Introduction

The atmospheric boundary layer (ABL) is the atmospheric region directly affected by the Earth's surface. The ABL height is variable and it depends on the specific geomorphology, the surface roughness and environment stratification of the region. It may extend to a few hundred meters to up to the radial distance of approximately 1 km above the Earth's surface. The study of the atmospheric boundary layer in wind tunnels plays an important role in many engineering applications. Usually, the ABL flow simulation in wind tunnels is applied to environmental studies and the investigation of the basic phenomena occurring in micro-meteorological atmosphere processes (Petersen, 2013). Furthermore, these researches help to solve problems of practical engineering interest, such as pollutant dispersion in complex terrain or urban areas, in which buildings produce different flow patterns (Baouabe *et al.*, 2011). Moreover, several other applications can be potentially benefited by

this kind of study, such as wind-farm energy production (Barriatto and Petry, 2018); development of infrastructure for overhead transmission lines in the electricity sector (Hamada *et al*., 2017); vibration assessment of structural cables (Jafari *et al*., 2020); assessment of the impact of atmospheric flow and stability on offshore oil platforms and large vessels (Liu *et al*., 2020); and external environments atmospheric flow evaluation of airborne disease dissemination, such as COVID-19 (Feng *et al*., 2020).

Wind tunnels are experimental facilities designed to simulate the airflow conditions. Similar studies can be performed in real environmental settings. After the experimental apparatus is built, it is necessary to evaluate the flow characteristics and analyze the flow patterns for which it was constructed (Al-Nehari *et al*., 2010). These experimental studies are the main knowledge sources for investigations that require an ABL profile. Recent techniques and facilities are continually developed with extensive research related to environmental and aerodynamic architectural structure issues (Cermak, 1995; Cermak *et al*., 1995; Abbaspour and Shojaee, 2009). An important step in the structural design process is to determine the effects of flow in high buildings, bridges, and other structures (ASCE, 2005). In addition, the simulation of an ABL profile has a key role in transport modeling and pollutant dispersion in the environment (Abdullah *et al*., 2007; Kho *et al*., 2007).

A series of experimental evaluations were conducted in the development of the ABL wind tunnel (Counihan, 1969, 1973; Cook, 1973; Irwin, 1981). The simulated characteristics of the boundary layers are consistent with the interpretation of measurements in real scale. In addition, studies of thermal stratification also have attracted scientific interest (Mahrt, 1999; Ohya, 2001; Pieterse and Harms, 2013; Mahrt, 2014). In this context, the use of spires in wind tunnels input for ABL simulation has become a common technique in experimental procedures of turbulent flows in external environments (Cermak, 1995; Cermak *et al*., 1995; Garg *et al*., 1997). Nevertheless, new techniques for observations and analysis are necessary to advance the comprehension of the atmospheric boundary layer (Mahrt, 2014, Lotfy *et al*. 2019).

Numerical simulations have been widely implemented as a comparison source of the phenomena associated with the atmospheric boundary layer. The computational results have shown an overall good agreement with experimental data (Ferreira *et al*., 1995; Athanassiadou and Castro, 2001). Additionally, numerical studies also help to obtain a preliminary understanding of the boundary layer development, it reduces the tunnel operating time and costs during the actual testing stage (Shojaee *et al*., 2014). The solution of the transport equations presents many difficulties due to its intrinsic non-linearity, therefore many numerical methodologies have been developed and are still being developed for this goal (Moraes *et al*. 2016, Chalhub *et al*. 2014 and 2014b). However, only a few articles presented numerical simulations on the thermally stratified ABL topic.

The current article presents numerical simulations and experimental measurements of the thermally stratified boundary layer. The experimental data are obtained from the atmospheric wind tunnel facility of the Laboratory of Characterization of Fluid Flow Dynamics that belongs to the Brazilian National Institute of Metrology, Quality and Technology (Inmetro). The wind tunnel configuration is composed of a transversal square section of 1m×1m and 10m in length. The flow velocity is controlled with a frequency inverter which turns a 9 kW fan, reaching a maximum approximate mean velocity of 10 m/s. Before entering the test section, the air crosses a diffuser (ratio 1:2), a set of screens and a honeycomb, respectively (Farias, *et al*., 2014). The mathematical model is solved using the OpenFOAM software (Jasak *et al*., 2007), which is an open-source library for Computational Fluid Dynamics (CFD). Two different spire set configurations and inlet velocities are considered. The main objective of this research is to evaluate the thermally stratified atmospheric boundary layer behavior for different configurations. Additionally, the numerical results are compared to the experimental data for validation purposes.

2. Mathematical formulation

The proposed problem is the analysis of the stratified airflow inside a wind tunnel considering two geometry configurations: three spires (3S) and four spires (4S), in which the 3S configuration can be seen in Figure 1. The spires have a base length of 0.0922m, a width of 0.015m, a height of 0.609m and the center distance among them is 0.25m and 0.2m for the 3S and 4S configurations, respectively. The tip of the spires was designed to be round, with a curvature diameter of 10% of the spire base length, to improve the quality of the generated mesh and simulation.

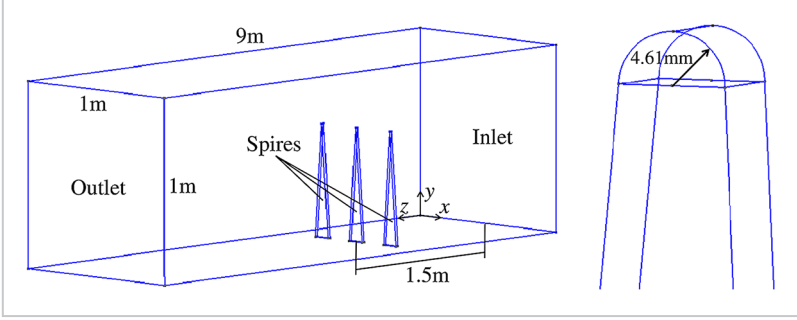

Figure 1 - Proposed problem geometry and tip of spires in detail.

For the simulation of the stratified airflow of the proposed problem, one needs to solve the coupled momentum, mass and energy equation. The airflow in the wind tunnel is modeled by partial differential equations describing the conservation of mass, momentum and energy in 3D Cartesian coordinates system for compressible flow. The governing equations for the flow, based on the Reynolds-averaged Navier–Stokes (RANS) approach with standard k-epsilon models are:

$$\nabla \cdot (\rho \mathbf{u}) = 0, \tag{1}$$

$$\nabla \cdot \left(\rho \mathbf{u} \mathbf{u} \right) = -\nabla p + \rho \mathbf{g} + \nabla \cdot \left(2 \mu_{eff} D(\mathbf{u}) \right) - \nabla \left(\frac{2}{3} \mu_{eff} \left(\nabla \cdot \mathbf{u} \right) \right), \tag{2}$$

$$\nabla \cdot \left(\rho \mathbf{u} h \right) + \nabla \cdot \left(\rho \mathbf{u} \frac{|\mathbf{u}|^2}{2} \right) = \nabla \cdot \left(\alpha_{eff} \nabla h \right) + \rho \mathbf{u} \cdot \mathbf{g}, \tag{3}$$

in which, the rate of strain tensor is defined as

$$D(\mathbf{u}) = \frac{1}{2} \left(\nabla \mathbf{u} + \left(\nabla \mathbf{u} \right)^T \right), \tag{4}$$

and μ_{eff} is the sum of the molecular and turbulent viscosity, ρ is the air density, $\mathbf{g}$ is the gravitational acceleration vector, p is pressure, $\mathbf{u}$ is velocity vector, h is the enthalpy. Additionally, the effective thermal diffusivity α_{eff} is the sum of laminar and turbulent thermal diffusivities:

$$\alpha_{eff} = \frac{\rho \nu_t}{Pr_t} + \frac{\mu}{Pr} = \frac{\rho \nu_t}{Pr_t} + \frac{k_T}{c_p} \tag{5}$$

where k_T is the thermal conductivity, c_p is the specific heat at constant pressure, μ is the dynamic viscosity, ν_t is the turbulent kinematic viscosity, Pr is the Prandtl number and Pr_t is the turbulent Prandtl number. The Reynolds stress components $\overline{u_i' u_j'}$ are parameterized as:

$$-\overline{u_i' u_j'} = \nu_t \left(\frac{\partial u_i}{\partial x_j} + \frac{\partial u_j}{\partial x_i} \right) - \frac{3}{2} k \delta_{ij} \tag{6}$$

$$\nu_t = C_\mu \frac{k^2}{\varepsilon} \tag{7}$$

where δ_{ij} is the Kronecker delta (δ=1, for $i = j$, otherwise =0), k is the turbulent kinetic energy, ε is the dissipation rate of the kinetic energy, and the C_μ is a constant having a value of 0.09. The turbulence kinetic energy, k, and its rate of dissipation, ε, are obtained from the following transport equations:

$$\frac{\partial}{\partial x_j} (k u_j) = \frac{\partial}{\partial x_j} \left(\frac{\nu_t}{\sigma_k} \frac{\partial k}{\partial x_j} \right) + \nu_t \left(\frac{\partial u_i}{\partial x_j} + \frac{\partial u_j}{\partial x_i} \right) \frac{\partial u_i}{\partial x_j} - \varepsilon \tag{8}$$

$$\frac{\partial}{\partial x_j} (\varepsilon u_j) = \frac{\partial}{\partial x_j} \left(\frac{\nu_t}{\sigma_\varepsilon} \frac{\partial \varepsilon}{\partial x_j} \right) + C_{1\varepsilon} \frac{\varepsilon}{k} \nu_t \left(\frac{\partial u_i}{\partial x_j} + \frac{\partial u_j}{\partial x_i} \right) \frac{\partial u_i}{\partial x_j} - C_{2\varepsilon} \frac{\varepsilon^2}{k} \tag{9}$$

where $\sigma_k = 1.0$ and $\sigma_\varepsilon = 1.3$ are turbulent Prandtl numbers for k and $C_{1\varepsilon} = 1.44$ and $C_{2\varepsilon} = 1.92$ are constants. The inlet velocity profile for the simulation is applied based on the experimental measurements in the tunnel entrance. It was employed uniform streamwise velocity and the turbulence kinetic energy k turbulent dissipation rate is:

$$k = 1.5 \, (IU)^2 \tag{10}$$

$$\varepsilon = \frac{C_\mu^{3/4} k^{3/2}}{0.07 L} \tag{11}$$

where I is the turbulence intensity of the flow at the entrance of the test section, and L is the characteristic length. The no-slip boundary conditions were used for the tunnel and spires wall. The boundary conditions for the velocity, pressure and temperature of the problem are shown below:

• Side and upper walls:

$$\mathbf{n}.\nabla p = 0 \quad (12)$$

$$\mathbf{u} = \mathbf{0} \quad (13)$$

$$\mathbf{n}.\nabla T = 0 \quad (14)$$

• Bottom wall:

$$\mathbf{n}.\nabla p = 0 \quad (15)$$

$$\mathbf{u} = \mathbf{0} \quad (16)$$

For the energy boundary condition, it is known that the heating element total power is $\dot{Q}_0 = 3.96$ kW and the total bottom surface area is $A = 9$ m², hence an approximate uniform heat flux can be written in the following form:

$$\dot{q}'' = \frac{\dot{Q}_0}{A}\eta = 0.264 kW/m^2 \quad (17)$$

where η is the heating element efficiency that represents the fraction of heat that actually enters the airflow. For this particular case $\eta = 0.6$.

• Inlet section:

$$\mathbf{n}.\nabla p = 0 \quad (18)$$

$$\mathbf{v} = V_{in}\,\hat{e}_z \quad (19)$$

$$T = T_{in} = 300\text{K} \quad (20)$$

• Outlet section:

$$p = 0 \quad 21)$$

$$\mathbf{n}.\nabla \mathbf{v} = \mathbf{0} \quad (22)$$

$$\frac{\partial T}{\partial z} = 0 \quad (23)$$

where **n** is the boundary orthonormal vector and **0** is the null vector.

In order to solve the turbulent flow, the k-epsilon turbulence model shown is utilized, which is the most common model used in computational fluid dynamics to simulate mean flow characteristics for turbulent flow conditions. It gives a general description of the flow by means of three transport equations.

3. Results

The spires are designed to obtain the required atmospheric boundary layer similarity within the test section of Inmetro's Wind Tunnel using the spire's design described by Shojaee *et al.* (2014). Subsequently, a computational analysis of the designed inlet configurations is performed using CFD in order to have an overall understanding of how well the inlet configurations could simulate the desired boundary layer conditions within the test section. The goal is to obtain a boundary layer characteristic after 7 m from the inlet. The numerical investigation was carried out using the buoyant SimpleFoam solver from OpenFOAM software version 3.0.1, based on a finite-volume discretization method and the geometry configurations were built in Gmsh-2.11.0 software. Table 1 presents the property values used for the current simulations.

Table 1 - Property values for simulation.

Input property parameters	
Specific heat at constant pressure (C_p)	1004.4 J/(kg K)
Dynamic viscosity (μ)	1.831×10^{-5} kg/(m s)
Gravitational acceleration (g)	9.81 m/s²
Molecular mass (m)	28.96
Prandtl (Pr)	0.705

Figure 2 illustrates the flow velocity for 3S spire configuration, and different cross-section downstream spires. It can be seen that the velocity is greatly impacted by the presence of the spires and this effect is key for emulating the stratified atmospheric boundary layer phenomenon.

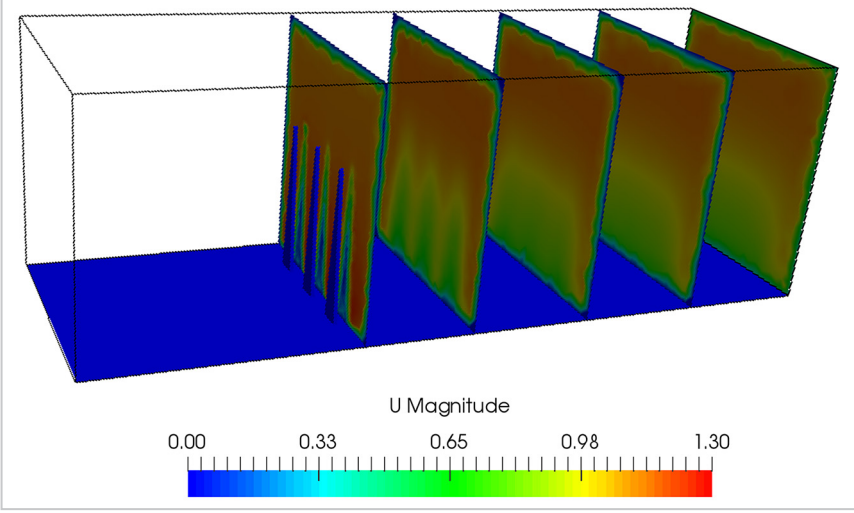

Figure 2 - Velocity magnitude for 3S configuration and V_{in} = 1.212.

In modeling of urban flow, a smaller grid size is desirable around the building model to better resolve the flow and dispersion field. A few mesh sizes were tested and the following optimum meshes with refined regions near spires are used for the present simulation: 389,867 and 404,867 tetrahedral cells for 3S and 4S configurations respectively. Moreover, two inlet velocities are chosen: 0.495 m/s and 1.212 m/s. For the collection of experimental data 20 thermocouples were positioned in the middle of the tunnel section (x = 0.5m) at 7 m downstream spires position.

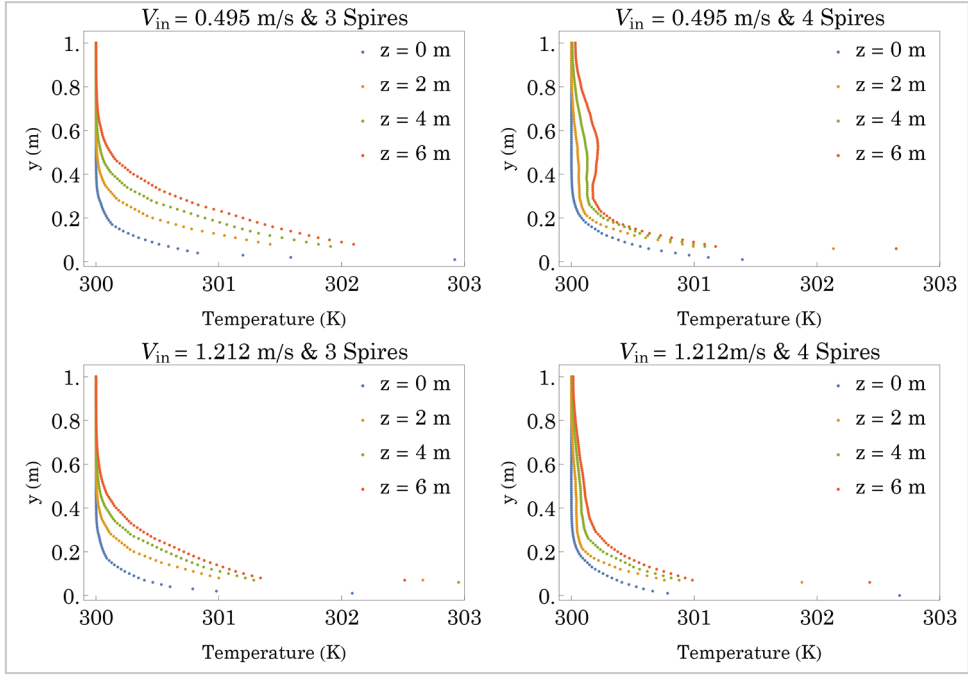

Figure 3 - Thermal boundary layer profiles for different streamwise positions, in which z = 0 is the spire position.

Figure 3 presents the thermal boundary layer for different velocities and spire configurations. Each figure presents temperature profiles related to different downstream positions, in which z = 0 is the spire's position. As can be observed in all cases, the thermal boundary layer thickness increases as the distance from the spires rises. This behavior is expected, since it is coherent with theoretical studies. When the number of spires increases, a greater region of the thermal profile is affected. Furthermore, increasing the inlet velocity generates a smoother temperature gradient.

Figure 4 shows a comparison between numerical and experimental data of the temperature profiles at z = 7 m. Although it is a difficult task to match experimental and theoretical data due to the enormous number of variables, one can note that the numerical results and measured data show a good overall agreement providing an acceptable thermal boundary layer profile for both spire geometries.

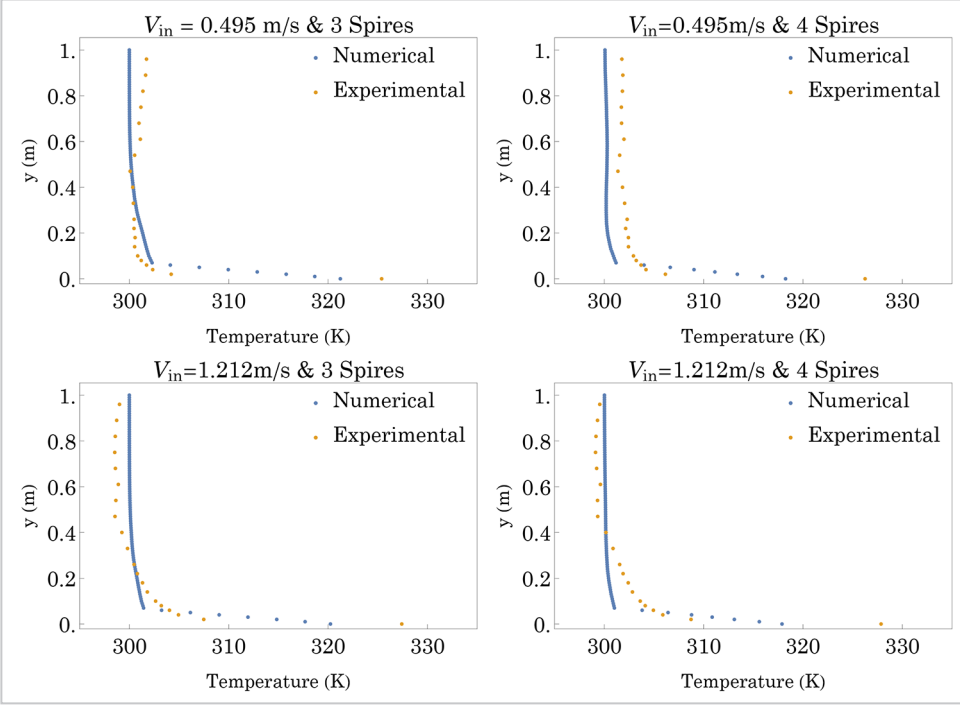

Figure 4 - Thermal boundary layer comparison between numerical and experimental data for *z* = 7m and *x* = 0.5 m, in which *z* = 0 is the spire position.

4. Conclusions

The current article has presented numerical simulations and experimental measurements of the thermally stratified boundary layer. The experimental data were obtained with Inmetro's atmospheric wind tunnel. In order to simulate the phenomenon and capture the features of the stratified flow, the compressible Navier-Stokes equations using the k-epsilon turbulence model are computed by buoyantSimpleFoam solver from OpenFOAM opensource software. Two different inlet velocities and spire sets were considered, in which a row of spires at the inlet of the wind tunnel was used to provide the appropriate stratified boundary layer, therefore emulating high-rise buildings.

The simulated and experimental results presented a good overall agreement and showed that the current configuration provides the desired thermal and dynamic stratified boundary layer necessary for the study of ABL. This research contributes to the thermally stratified atmospheric boundary layer understanding and its mathematical predictions. Moreover, this kind of numerical simulation also helps to reduce the wind tunnel operation time and costs.

Acknowledgements

The authors would like to acknowledge the financial support provided by CNPq, CAPES and FAPERJ, Brazilian agencies for the fostering of sciences, and Inmetro.

References

ABBASPOUR, M.; SHOJAEE, M. Innovative approach to design a new national low speed wind tunnel. ***International Journal of Environmental Science & Technology,*** v. 6, n. 1, p. 23–34, 2009.

ABDULLAH, L. C.; WONG, L. L.; SAARI, M.; SALMIATON, A.; RASHID, M. S. A. Particulate matter dispersion and haze occurrence potential studies at a local palm oil mill. ***International Journal of Environmental Science & Technology,*** v. 4, n. 2, p. 271–278, 2007.

AL-NEHARI, H. A.; ABDEL-RAHMAN, A. K.; SHAFEY, H. M.; NASSIB, A. E. Characterization of a low-speed

wind tunnel simulating urban atmospheres. ***Journal of Engineering Sciences,*** v. 38, n. 32, p. 509–532, 2010.

AMERICAN SOCIETY OF CIVIL ENGINEERS. ***Minimum design loads for buildings and other structures.*** Reston, Virginia: ASCE, 2005. v. 7.

ATHANASSIADOU, M.; CASTRO, I. P. Neutral flow over a series of rough hills: a laboratory experiment. ***Boundary layer meteorology,*** v. 101, p. 1–30, 2001.

BAOUABE, I. B.; BOURNOT, H.; SAID, N. M.; MHIRI, H.; LE PALEC, G. Experimental and numerical analysis of the jet dispersion from a bent chimney around an obstacle. ***Heat and Mass Transfer,*** v. 47, n. 3, p. 323-342, 2011.

BARRIATTO, L. C.; PETRY, A. P. Modelagem do escoamento termicamente estratificado na camada limite atmosférica. *In*: CONGRESSO BRASILEIRO DE ENERGIA SOLAR, 7., Gramado, Brazil, 2018. ***Anais*** [...]. Gramado: ABENS, 2018.

CERMAK, J. E. Progress in physical modeling for wind engineering. ***Journal of Wind Engineering and Industrial Aerodynamics,*** v. 54, p. 439–455, 1995.

CERMAK, J. E.; COCHRAN, L. S.; LEFLIER, R. D. Wind-tunnel modelling of the atmospheric surface layer. ***Journal of Wind Engineering and Industrial Aerodynamics,*** v. 54, p. 505–513, 1995.

CHALHUB, D. J. N. M.; SPHAIER, L. A.; ALVES, L. S. B. Integral transform analysis of Poisson problems that occur in discrete solutions of the incompressible Navier-Stokes equations. ***Journal of Physics: Conference Series,*** v. 547, n. 1, 2014.

CHALHUB, D. J. N. M.; SPHAIER, L. A.; ALVES, L. S. B. Semi-analytical method for the solution of the Poisson equation derived from the Navier-Stokes using integral transforms. *In*: ASME 2014 - INTERNATIONAL CONFERENCE ON NANOCHANNELS, MICROCHANNELS, AND MINICHANNELS, 12th, 2014, Chicago, Illinois, USA. ***Proceedings*** […]. Chicago: ASME, 2014b.

COOK, N. On simulating the lower third of the urban adiabatic boundary layer in a wind tunnel. ***Atmospheric Environment (1967),*** v. 7, n. 7, p. 691–705, 1973.

COUNIHAN, J. An improved method of simulating an atmospheric boundary layer in a wind tunnel. Atmospheric Environment (1967), v. 3, n. 2, p. 197–214, 1969.

COUNIHAN, J. Simulation of an adiabatic urban boundary layer in a wind tunnel. ***Atmospheric Environment (1967),*** v. 7, n. 7, p. 673–689, 1973.

FARIAS, M. H.; SANTOS, A. M.; SOUZA, D. B.; FERREIRA, L. L. R.; MASSARI, P. L.; MASSARI, P. L.; GARCIA, D. A.; COSTA, F. O. Characterization of low speed atmospheric wind tunnel. *In*: INTERNATIONAL CONGRESS ON MECHANICAL METROLOGY, 3rd, CIMMEC2014, Gramado, Brazil, 2014. ***Proceedings*** […]. Gramado: CIMMEC, 2014.

FENG, Y.; MARCHAL, T.; SPERRY, T.; YI, H. Influence of wind and relative humidity on the social distancing effectiveness to prevent COVID-19 airborne transmission: a numerical study. ***Journal of aerosol science,*** v. 147, 105585, 2020.

FERREIRA, A.; LOPES, A.; VIEGAS, D.; SOUSA, A. Experimental and numerical simulation of flow around two-dimensional hills. ***Journal of wind engineering and industrial aerodynamics,*** v.54, p. 173–181, 1995.

GARG, R.; LOU, J.; KASPERSKI, M. Some features of modeling spectral characteristics of flow in boundary layer wind tunnels. ***Journal of wind engineering and industrial aerodynamics,*** v. 72, p. 1–12, 1997.

HAMADA, A.; KING, J. P. C.; EL DAMATTY, A. A.; BITSUAMLAK, G.; HAMADA, M. The response of a guyed transmission line system to boundary layer wind. Engineering Structures, v.139, p. 135-152, 2017.

IRWIN, H. The design of spires for wind simulation. ***Journal of Wind Engineering and Industrial Aerodynamics,*** v. 7, n. 3, p. 361–366, 1981.

JAFARI, M.; HOU, F.; ABDELKEFI, A. Wind-induced vibration of structural cables. ***Nonlinear Dynamics,*** v. 100, n. 5, p. 1-71, 2020.

JASAK, H.; JEMCOV, A.; TUKOVIC, Z. OpenFOAM: a C++ library for complex physics simulations. *In*: INTERNATIONAL WORKSHOP ON COUPLED METHODS IN NUMERICAL DYNAMICS, Dubrovnik, Croatia, 2007. ***Proceedings*** […]. Dubrovnik: IUC, 2007. v. 1000.

KHO, W. L. F.; SENTIAN, J.; RADOJEVIC, M.; TAN, C. L.; LAW, P. L.; HALIPAH, S. Computer simulated versus observed no2 and so2 emitted from elevated point source complex. ***International Journal of Environmental Science & Technology,*** v. 4, n. 2, p. 215–222, 2007.

LIU, G.; SUN, Y.; ZHONG, B.; XIE, Y.; INCECIK, A.; LI, Z. Analysis of wind load effect on key components in a jack-up offshore platform. ***Applied Ocean Research,*** v. 101, 102263, 2020.

LOTFY, E. R.; ABBAS, A. A.; ZAKI, S. A. et al. Characteristics of turbulent coherent structures in atmospheric flow under different shear–buoyancy conditions. ***Boundary-Layer Meteorology,*** v. 173, p. 1-27, 2019.

MAHRT, L. Stratified atmospheric boundary layers. ***Boundary-Layer Meteorology,*** v. 90, n. 3, p.375–396, 1999.

MAHRT, L. Stably stratified atmospheric boundary layers. ***Annual Review of Fluid Mechanics,*** v. 46, p. 23–45, 2014.

MORAES, G.; TEIXEIRA, R. S.; ALVES, L. S. B. Validity of parametric restrictions to the modified Buckley--Leverett equations. ***Journal of Porous Media,*** v.19, n.9, p. 811-819, 2016.

OHYA, Y. Wind-tunnel study of atmospheric stable boundary layers over a rough surface. Boundary-***Layer Meteorology,*** v. 98, n. 1, p. 57–82, 2001.

PETERSEN, G. ***Wind tunnel modelling of atmospheric boundary layer flow over hills.*** 2013. 303f. Thesis (Ph.D.) –

Universität Hamburg, Hamburg, 2013.

PIETERSE, J. E.; HARMS, T. CFD investigation of the atmospheric boundary layer under different thermal stability conditions. ***Journal of Wind Engineering and Industrial Aerodynamics,*** v. 121, p. 82–97, 2013.

SHOJAEE, S. M. N.; UZOL, O.; KURÇ, Ö. Atmospheric boundary layer simulation in a short wind tunnel. International ***Journal of Environmental Science and Technology,*** v. 11, n. 1, p. 59–68, 2014.

Received: 30 March 2020 - Accepted: 24 September 2020.